

Robust control of a two-state Greitzer compressor model by state-feedback linearization

Christoph Josef Backi¹, Jan Tommy Gravdahl² and Sigurd Skogestad¹

Abstract—In this paper we introduce an anti surge controller for a close-coupled valve (CCV) in a compression system. The controller is based upon feedback linearization in combination with linear state feedback. The mentioned CCV modifies the characteristics of the compressor, allowing it to be stably operated beyond the original surge line. It is shown that the original model consisting of the compressor in combination with the CCV can be transformed into the Byrnes-Isidori-Normalform, a necessity in order to enable feedback linearization. Furthermore, robustness of the controller is illustrated by circle criterion analysis with a sector nonlinearity feedback. Simulation examples illustrate the theoretical robustness investigation also for the case when the control signal is bounded and noise is added to the state derivatives and to the output.

I. INTRODUCTION

In this paper we propose a nonlinear controller for the control of a model of an axial compressor introduced by [6]. If a compression system is operated below a certain mass flow limit (denoted surge line), it will go into a marginally stable, potentially unstable mode of operation. This mode results in undesired limit-cycle oscillations in flow and pressure, so called surge, which can lead to physical damage of the compression system or at least to reduction in performance.

Therefore, controlling the occurrence of surge is vital to avoid damages and keep the performance up. One alternative of active surge control is the use of a so called close-coupled valve (CCV), as introduced by [11]. The CCV acts on the compressor's characteristics directly and thereby stabilizes the system. The overall dynamics of the compressor in combination with the CCV can be considered as those of an extended compressor, see Figure 1.

There exist many works concerning the control of surge in compression systems, such as control by state feedback as well as output feedback control. [4] implemented a control structure based upon a CCV controlled by backstepping methods. In [9] an output feedback design for a Moore-Greitzer compressor model was introduced, whereas in [10] a robust output feedback controller for active surge control of compression systems was presented. The authors of [12] developed a control system based upon piston actuation to actively control surge. In [13] a back-up for failure of the

active surge control is introduced. Broad reviews of surge and rotating stall controllers can be found in [3] and [5].

The aforementioned article [4] introduces surge control using feedback from mass flow. Due to the fact that mass flow is both difficult and expensive to measure, mass flow observers have been studied, e.g. in [2], [9] and [10] for more general compression systems. An observer for the Greitzer compressor model considered in this work has been presented in [1] providing a full state observer with local stability results based on a circle criterion design superior to for example an Extended Kalman Filter design, especially in the surge case.

Not only Jacobian-based linearization around a given setpoint can deliver satisfactory results when designing a controller for a nonlinear system. Also feedback linearization can be applicable in some cases. The advantage over Jacobian-based linearization is that the linearized system not only holds for a specific setpoint, but at least for a whole family of setpoints or even the whole feasible state-space. Especially when the dynamics of the system are well modeled and understood, feedback linearization can be applied, but also if the model diverges from the real process.

We will demonstrate that the feedback linearization methodology can successfully be used to stabilize surge in a compression system. This will be done by theoretical robustness analysis incorporating a circle criterion investigation with a sector nonlinearity feedback as well as illustrated by simulation examples.

The paper is structured as follows: In Section II the mathematical model of the compression system is introduced, whereas Section III provides the controller design with robustness analysis. Section IV presents some illustrative simulation examples while the paper is closed with the conclusion in Section V.

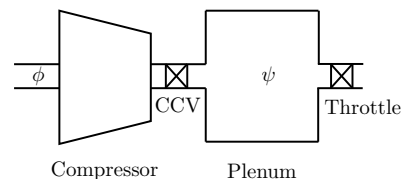


Fig. 1. Schematic representation of a compressor with CCV, ψ indicates non-dimensional pressure and ϕ denotes non-dimensional flow

II. MATHEMATICAL MODEL

The dynamics of the two-state Greitzer compressor model in combination with a close-coupled valve (CCV) for the

¹C. J. Backi (corresponding author) and S. Skogestad are with the Department of Chemical Engineering, Norwegian University of Science and Technology, N-7491 Trondheim, Norway {christoph.backi, sigurd.skogestad}@ntnu.no

²J. T. Gravdahl is with the Department of Engineering Cybernetics, Norwegian University of Science and Technology, N-7491 Trondheim, Norway jan.tommy.gravdahl@ntnu.no

control of compressor surge can be considered as those of an extended compressor with the CCV pressure drop acting as part of an equivalent compressor. The following dimensionless equations hold for the compressor (plant) with the origin as equilibrium point

$$\begin{aligned}\dot{\hat{\psi}} &= \frac{1}{B} \left(\hat{\phi} - \hat{\Phi}(\hat{\psi}) \right) \\ \dot{\hat{\phi}} &= B \left(\hat{\Psi}_c(\hat{\phi}) - \hat{\psi} - u \right),\end{aligned}\quad (1)$$

where u is the pressure drop across the CCV,

$$\hat{\Phi}(\hat{\psi}) = \gamma \left(\text{sgn}(\hat{\psi} + \psi_0) \sqrt{|\hat{\psi} + \psi_0|} - \sqrt{\psi_0} \right)$$

indicates the throttle characteristics and

$$\hat{\Psi}_c(\hat{\phi}) = -k_3 \hat{\phi}^3 - k_2 \hat{\phi}^2 - k_1 \hat{\phi},$$

denotes the compressor characteristics.

Be advised that $\hat{\cdot}$ does not label an estimated value, but the deviation from operating points $\hat{\psi} = \psi - \psi_0$ and $\hat{\phi} = \phi - \phi_0$, respectively. ϕ designates the non-dimensional mass flow $\left(\phi = \frac{\dot{m}}{\rho U A_c} \right)$, whereas ψ indicates the non-dimensional pressure $\left(\psi = \frac{p}{0.5 \rho U^2} \right)$ and γ denotes the throttle gain. Note furthermore that $\text{sgn}(0) = 0$, that time has been normalized by the Helmholtz frequency, thus $\tau = t \omega_H$, and that the pressure drop across the CCV typically only can provide positive pressure differences, meaning that $u \geq 0$. This is based on the fact that the CCV should be fully opened in the equilibrium point. However, it can be operated as an initially throttled valve, which will lower the performance of the overall compression system.

For the parameters it holds that $B = \frac{U}{2a_s} \sqrt{\frac{V_p}{A_c L_c}} > 0$, where U is the compressor blade tip speed, a_s is the speed of sound, V_p is the plenum volume, A_c is the flow area and L_c is the length of ducts and compressor, $k_1 = \frac{3H\phi_0}{2W^2} \left(\frac{\phi_0}{W} - 2 \right)$, $k_2 = \frac{3H}{2W^2} \left(\frac{\phi_0}{W} - 1 \right)$ and $k_3 = \frac{H}{2W^3}$, where $H > 0$, $W > 0$ and $\phi_0 > 0$. The operating point ψ_0 can be calculated via $\psi_0(\phi_0) = \psi_{0c} + H \left[1 + \frac{3}{2} \left(\frac{\phi_0}{W} - 1 \right) - \frac{1}{2} \left(\frac{\phi_0}{W} - 1 \right)^3 \right]$ with $\psi_{0c} = 0.3$ and the throttle gain γ via $\gamma = \frac{\phi_0}{\sqrt{\psi_0}}$ (see [4]).

By setting $\hat{\psi} = x_1$, $\hat{\phi} = x_2$, $\psi_0 = x_{10}$, the system (1) can be rewritten as

$$\begin{aligned}\dot{x}_1 &= \frac{1}{B} \left[x_2 - \gamma \left(\text{sgn}(x_1 + x_{10}) \sqrt{|x_1 + x_{10}|} - \sqrt{x_{10}} \right) \right] \\ \dot{x}_2 &= B \left(-k_3 x_2^3 - k_2 x_2^2 - k_1 x_2 - x_1 - u \right),\end{aligned}\quad (2)$$

which is in fact a representation of a nonlinear system in the form $\dot{x} = a(x) + b(x)u$ with

$$\begin{aligned}a(x) &= \begin{bmatrix} \frac{1}{B} \left[x_2 - \gamma \left(\text{sgn}(x_1 + x_{10}) \sqrt{|x_1 + x_{10}|} - \sqrt{x_{10}} \right) \right] \\ B \left(-k_3 x_2^3 - k_2 x_2^2 - k_1 x_2 - x_1 \right) \end{bmatrix} \\ b(x) &= \begin{bmatrix} 0 \\ -B \end{bmatrix}.\end{aligned}$$

III. CONTROLLER DESIGN

In this Section we are going to investigate and present the controller design based on the principle of feedback linearization. Thereby we will conduct a transformation of the system (2) into the *Byrnes-Isidori-Normalform* (B-I-NF) as well as a full state linearization / state feedback linearization. The theory behind this investigation is introduced and outlined in e.g. [7] and [8].

A. Transformation

It can be seen, that the system (2) is nonlinear in both differential equations. In order to conduct feedback linearization, the system will be transformed into the B-I-NF, which represents the actual nonlinear system of order n by a chain of n integrators and only one nonlinearity appearing in the n^{th} derivative of the new state variable in the transformed coordinates \hat{z}_n . A necessity for this procedure is to have a relative degree of $r = n$, meaning that the input may first appear in the n^{th} derivative of the output y . In case of $r < n$, the integrator chain will reduce to r integrators and the remaining $n - r$ states will be represented as the internal, non-observable zero dynamics, which must be stable in order to conduct feedback linearization.

1) *Relative Degree*: As outlined before, it is easier, cheaper and more practical to measure the pressure in compression systems. Therefore, (2) has the defined output

$$y = h(x) = x_1. \quad (3)$$

With regards to full state feedback control there exist observers for the system (2), as outlined in Section I. The output (3) leads to a relative degree of $r = n = 2$ as can be shown as follows by calculating the derivative of the output with respect to time

$$\begin{aligned}\dot{y} &= \dot{x}_1, \\ \ddot{y} &= \ddot{x}_1 = \frac{1}{B} \left[\dot{x}_2 - \gamma \dot{x}_1 p_1(x_1, x_{10}) \right] \\ &= -k_3 x_2^3 - k_2 x_2^2 - k_1 x_2 - x_1 - u \\ &\quad - \frac{\gamma p_1}{B^2} \left[x_2 - \gamma \left(\text{sgn}(x_1 + x_{10}) \sqrt{|x_1 + x_{10}|} - \sqrt{x_{10}} \right) \right],\end{aligned}\quad (4)$$

where

$$p_1 = p_1(x_1, x_{10}) = \text{sgn}(x_1 + x_{10}) \frac{x_1 + x_{10}}{2|x_1 + x_{10}|^{\frac{3}{2}}}.$$

As we can see, the input appears in the second derivative of the output with respect to time, and thus $r = n$. This means that the system (2) will not have any zero dynamics in the B-I-NF.

2) *Byrnes-Isidori-Normalform*: The state transformation for a system with relative degree of $r = n = 2$ is defined as

$$\begin{bmatrix} z_1 \\ z_2 \end{bmatrix} = \begin{bmatrix} h(x) \\ L_a h(x) \end{bmatrix} = T(x), \quad (5)$$

where $L_a h(x)$ is the Lie-derivative of $h(x)$ along $a(x)$

$$L_a h(x) = \frac{\partial h(x)}{\partial x} a(x) = \begin{bmatrix} 1 & 0 \end{bmatrix} \begin{bmatrix} \dot{x}_1 \\ \dot{x}_2 \end{bmatrix} = \dot{x}_1. \quad (6)$$

By putting (3) and (6) into (5) we obtain

$$\begin{bmatrix} \dot{z}_1 \\ \dot{z}_2 \end{bmatrix} = \begin{bmatrix} x_1 \\ \frac{1}{B} \left[x_2 - \gamma \left(\text{sgn}(x_1 + x_{1_0}) \sqrt{|x_1 + x_{1_0}|} - \sqrt{x_{1_0}} \right) \right] \end{bmatrix} \quad (7)$$

which leads to the following differential equations

$$\begin{bmatrix} \dot{z}_1 \\ \dot{z}_2 \end{bmatrix} = \begin{bmatrix} \dot{x}_1 \\ \dot{x}_2 \end{bmatrix} = \begin{bmatrix} z_2 \\ \ddot{y} \end{bmatrix}. \quad (8)$$

Out of (7) we obtain

$$\begin{bmatrix} x_1 \\ x_2 \end{bmatrix} = \begin{bmatrix} z_1 \\ p_2(z_1, z_2, x_{1_0}) \end{bmatrix} = \begin{bmatrix} z_1 \\ p_2 \end{bmatrix}, \quad (9)$$

where we have used the shorthand

$$p_2 = Bz_2 + \gamma \left(\text{sgn}(z_1 + x_{1_0}) \sqrt{|z_1 + x_{1_0}|} - \sqrt{x_{1_0}} \right).$$

By putting (9) into (4) and afterwards putting the result of this into (8), we receive

$$\begin{aligned} \dot{z}_1 &= z_2 \\ \dot{z}_2 &= -k_3 p_2^3 - k_2 p_2^2 - k_1 p_2 - z_1 - u - \frac{\gamma z_2}{B} p_1(z_1, x_{1_0}), \end{aligned} \quad (10)$$

which represents the transformation of the original system (2) in B-I-NF.

B. Full State Linearization

The state feedback linearization is possible, iff the B-I-NF can be represented in the form

$$\begin{aligned} \dot{z} &= A_{bi} z + B_{bi} \theta(x) [u - \sigma(x)] \\ y &= C_{bi} z, \end{aligned} \quad (11)$$

and furthermore if the pair (A_{bi}, B_{bi}) is controllable as well as $\theta(x)$ being nonsingular. Therefore we calculate the functions $\sigma(x)$ and $\theta(x)$ as

$$\begin{aligned} \theta(x) &= L_b L_a h(x) = \frac{\partial (L_a h(x))}{\partial x} b(x) \\ &= \begin{bmatrix} -\frac{\gamma}{B} p_1(x_1, x_{1_0}) & \frac{1}{B} \end{bmatrix} \begin{bmatrix} 0 \\ -B \end{bmatrix} = -1 \\ \sigma(x) &= -\frac{L_a^2 h(x)}{L_b L_a h(x)} = \frac{\partial (L_a h(x))}{\partial x} a(x) \\ &= \begin{bmatrix} -\frac{\gamma}{B} p_1(x_1, x_{1_0}) & \frac{1}{B} \end{bmatrix} a(x) \\ &= -k_3 x_2^3 - k_2 x_2^2 - k_1 x_2 - x_1 \\ &\quad - \frac{\gamma p_1}{B^2} \left[x_2 - \gamma \left(\text{sgn}(x_1 + x_{1_0}) \sqrt{|x_1 + x_{1_0}|} - \sqrt{x_{1_0}} \right) \right] \end{aligned}$$

and see that $\theta(x)$ is nonsingular and that $\sigma(x)$ corresponds with $\ddot{x}_1 + u$, where \ddot{x}_1 is defined in (4).

This leads to the matrices

$$A_{bi} = \begin{bmatrix} 0 & 1 \\ 0 & 0 \end{bmatrix}, \quad B_{bi} = \begin{bmatrix} 0 \\ 1 \end{bmatrix}, \quad [B_{bi} \quad A_{bi} B_{bi}] = \begin{bmatrix} 0 & 1 \\ 1 & 0 \end{bmatrix}$$

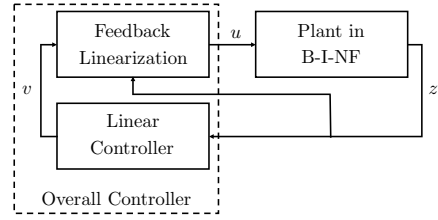


Fig. 2. System representation for controller design

where latter is the controllability matrix, which has full rank. Hence, the original system, respectively the transformed system, can be represented in the form (11).

In Figure 2 the final scheme for controller design can be seen. It incorporates the transformation of the nonlinear system (2) in B-I-NF, as well as the controller consisting of the feedback linearization and a linear state feedback controller.

C. State Feedback Linearization

So far, we have achieved to transform the original system (2), which has nonlinearities in both state equations, into a system that has nonlinearities only in one state equation (10). Furthermore, we have shown that the system is state feedback linearizable (11). The feedback linearization is now performed by finding an expression for the input u , in order to cancel out the nonlinearities and obtain a new input v . Linear expressions can be moved into the A_{bi} matrix.

Feedback linearization requires exact model knowledge. However, parameters of a mathematical model are always uncertain, and we proceed to account for this uncertainty by performing a robustness analysis of the closed loop system.

We choose the feedback u

$$u = -\check{k}_3 p_2^3 - \check{k}_2 p_2^2 - \check{k}_1 p_2 - \frac{\gamma z_2}{B} p_1(z_1, x_{1_0}) + v, \quad (12)$$

where \check{k}_i denote the parameters that are chosen in the controller. Hence we obtain the following closed loop form

$$\begin{aligned} \dot{z}_1 &= z_2 \\ \dot{z}_2 &= (\check{k}_3 - k_3) p_2^3 + (\check{k}_2 - k_2) p_2^2 + (\check{k}_1 - k_1) p_2 - z_1 - v. \end{aligned} \quad (13)$$

The closed-loop system (13) consists therefore of a linear part controlled with the state-feedback v and a nonlinear part in the second state-derivative \dot{z}_2 , which can be interpreted as a sector nonlinearity feedback $f_1(p_2)$ as shown in Figure 3. As can be seen, if the parameter values k_i are known exactly, meaning $\check{k}_i \equiv k_i$, the sector nonlinearity becomes zero and we obtain a purely linear system.

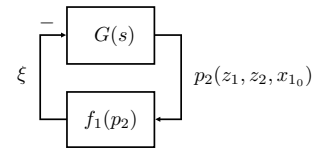


Fig. 3. The principle of a sector nonlinearity feedback

Thus, with the linear feedback

$$v = K_1 z_1 + K_2 z_2, \quad (14)$$

(13) can be written as

$$\begin{aligned} \begin{bmatrix} \dot{z}_1 \\ \dot{z}_2 \end{bmatrix} &= \underbrace{\begin{bmatrix} 0 & 1 \\ -1 - K_1 & -K_2 \end{bmatrix}}_{A_{lin}} \begin{bmatrix} z_1 \\ z_2 \end{bmatrix} + \underbrace{\begin{bmatrix} 0 \\ 1 \end{bmatrix}}_{B_{lin}} (-\xi), \\ y &= \underbrace{\begin{bmatrix} 1 & 0 \end{bmatrix}}_{C_{lin}} \begin{bmatrix} z_1 \\ z_2 \end{bmatrix}, \end{aligned} \quad (15)$$

where

$$\xi = f_1(p_2) = (k_3 - \check{k}_3)p_2^3 + (k_2 - \check{k}_2)p_2^2 + (k_1 - \check{k}_1)p_2. \quad (16)$$

Absolute stability of (15) can be ensured by circle criterion analysis, which states that (16) must be lower and upper bounded in the sectors I and III in the $(p_2, f_1(p_2))$ -plane. This can be achieved by requiring $k_3 - \check{k}_3 > 0$, meaning that \check{k}_3 of the controller should be chosen small compared to k_3 of the plant model and, in addition, that (16) should be nondecreasing, meaning that $\frac{df_1(p_2)}{dp_2} = 0$ shouldn't have any real solutions. This can be obtained by adding a term ηp_2 to the control law (12) and consequently to (16) yielding

$$\frac{df_1(p_2)}{dp_2} = 3(k_3 - \check{k}_3)p_2^2 + 2(k_2 - \check{k}_2)p_2 + \eta + (k_1 - \check{k}_1),$$

resulting in a bound for η

$$\eta > \frac{(k_2 - \check{k}_2)^2}{3(k_3 - \check{k}_3)} - (k_1 - \check{k}_1), \quad (17)$$

which was obtained by requiring the radicand of the solutions of $\frac{df_1(p_2)}{dp_2} = 0$ to be negative. We can rewrite (17) in terms of the coefficients H , W , \check{H} and \check{W} (see Section II for the definitions of the parameters k_i), and obtain

$$\eta > \frac{3}{2} \frac{(H\check{W}^2 - \check{H}W^2)^2}{W\check{W}(H\check{W}^3 - \check{H}W^3)}.$$

We can only allow positive values for η as negative values would imply that the shape of (16) changes. Hence, we must require $H\check{W}^3 > \check{H}W^3$ meaning to choose \check{W} sufficiently big and \check{H} sufficiently small, which corresponds with choosing \check{k}_3 sufficiently small. Hence, $f_1(p_2) \in [\alpha, \beta]$, where $0 < \alpha < \beta$ and $[\alpha, \beta]$ describes a sector created by the two linear functions αp_2 and βp_2 .

In addition, in order to guarantee absolute stability of (15), the transfer function

$$G(s) = C_{lin}(sI - A_{lin})^{-1}B_{lin} = \frac{1}{s^2 + K_2s + K_1 + 1}$$

must be Hurwitz and the transfer function

$$\tilde{G}(s) = \frac{1 + \beta G(s)}{1 + \alpha G(s)} = \frac{s^2 + K_2s + K_1 + \beta + 1}{s^2 + K_2s + K_1 + \alpha + 1} \quad (18)$$

has to be strictly positive real.

The transfer function (18) is strictly positive real iff the following two conditions hold

$$\begin{aligned} \tilde{G}(\infty) &> 0, \\ \operatorname{Re}[\tilde{G}(j\omega)] &> 0, \end{aligned} \quad (19)$$

where the expression for (20) is given in (24) at the end of this article. We can directly see that (19) is automatically fulfilled as $\tilde{G}(\infty) = 1$. The second condition (20), however, is only fulfilled for specific values of $\alpha > 0$ and $\beta > 0$ as well as $K_1 > 0$ and $K_2 > 0$, which in addition should render $\tilde{G}(s)$ Hurwitz. Thereby the choice of $\alpha > 0$ and $\beta > 0$ is dictated by the shape of (16) and thus by the choice of \check{H} and \check{W} . It holds that, the bigger the parameter \check{k}_3 will be chosen, the bigger η and β and the smaller α have to be chosen. For β big and α small, the feedback gains $K_1 > 0$ and $K_2 > 0$ will have to be chosen large in order to compensate for the poor choice of \check{k}_3 . The solutions of $\operatorname{Re}[\tilde{G}(j\omega)] = 0$ are $\omega_i, i = 1, 2, 3, 4$, which should be complex in order for (18) to be strictly positive real. The expressions for ω_i are given in (25) at the end of this article as well.

Nevertheless, it must be mentioned that by examining the marginally stable surge dynamics of the system (see Figure 7), a local stability result is sufficient, which limits the size of β and thus of the feedback gains K_1 and K_2 significantly.

The control law hence looks like

$$u = -\check{k}_3 p_2^3 - \check{k}_2 p_2^2 - (\check{k}_1 - \eta)p_2 - \frac{\gamma z_2}{B} p_1(z_1, x_{10}) + v. \quad (21)$$

D. Alternative Formulation

In theory there is an even more robust way to design the controller, namely by choosing the control signal as

$$u = \check{k}_3 p_2^3 + \check{k}_2 p_2^2 + (\check{k}_1 + \eta)p_2 - \frac{\gamma z_2}{B} p_1(z_1, x_{10}) + v, \quad (22)$$

yielding the same structure as in (15), but with

$$\xi = f_2(p_2) = (k_3 + \check{k}_3)p_2^3 + (k_2 + \check{k}_2)p_2^2 + (k_1 + \check{k}_1 + \eta)p_2. \quad (23)$$

Now we see that there are no restrictions on the choice of \check{k}_3 as the sum $k_3 + \check{k}_3$ will always be positive. We can employ the same procedure as before by adding a term ηp_2 to the control law, leading to the bound on η

$$\eta > \frac{3}{2} \frac{(H\check{W}^2 + \check{H}W^2)^2}{W\check{W}(H\check{W}^3 + \check{H}W^3)}.$$

Hence, if we choose any feasible values for \check{H} and \check{W} , we can find a sufficiently large constant η such that the sector nonlinearity (23) is nondecreasing, i.e. $f_2(p_2) \in [\alpha, \beta]$. However, this will require very large values for the linear state feedback gains K_1 and K_2 in order to fulfill (20) and make (18) strictly positive real. Thus this approach will not be applicable in practice. Therefore we concentrate on the initial formulation of the control law (21) in the simulations.

E. Implementation

The control law (21) can be directly implemented to the original system (2) by expressing the states z_1 and z_2 by their respective formulations in x -coordinates as stated in (7). The scheme can be seen in Figure 4.

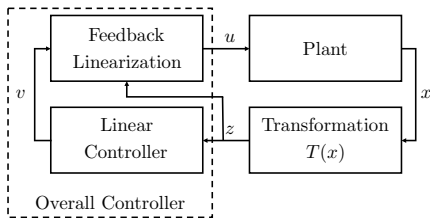


Fig. 4. Controller implementation on the real system, where the state vector x is assumed measurable, Feedback Linearization (22), Linear Controller (14), Plant (2) and Transformation (5)

IV. SIMULATIONS

In this Section we are going to present simulation results for different cases in order to demonstrate the robust nature of the controller. As mentioned before, the system is quite limited in actuation since the CCV can only provide positive pressure drops. Hence, only positive control signals are available and in addition, the maximal pressure drop is defined not to exceed 0.2. This is realized by introducing upper and lower bounds on the control signal, $0 \leq u \leq 0.2$. Furthermore, the maximal rate of change of the control signal is defined to be ± 0.5 in order to take actuation dynamics into account. The simulation parameters are listed in the Appendix, except for values that will change from simulation to simulation. These will be listed below the respective Figures.

For the state feedback it is assumed that all states are measurable. However, as pointed out before, there exist observers for the estimation of nonmeasurable states, see e.g. [1] or [2]. Furthermore, we will add white Gaussian noise to both state derivatives and to the output $y = x_1$ in order to take modeling as well as measurement errors into account. The white Gaussian noise is incorporated to the simulations in MATLAB[®] Simulink as band-limited white noise with a sample time of 0.01, a seed of 0 and noise powers of 10^{-6} and 10^{-7} , respectively. State feedback is rather noise-sensitive and can be minimized using a filter. An observer can for example be used not just to estimate the non-measurable state x_2 , but also to obtain a smoothed signal for the measurement x_1 . For all simulations that follow it holds that the systems starts in the stable region of the compressor map, namely at $\phi_0 = 0.6$, however, at $\tau = 10$ the operating point is changed to $\phi_0 = 0.3$, which is in the surge area. The controller is turned on at $\tau = 30$.

In Figure 5 we are going to present two simulations investigating two noise powers and their influence on the overall stabilization. In the top left plot a simulation result for a noise power of 10^{-6} is presented, whereas a result for a noise power of 10^{-7} is shown in the top right plot. The respective control signals are shown below each plot and, as can be seen, for larger noise powers the stabilization of the system takes longer.

For the following simulations we will choose the noise power to be 10^{-7} .

Figure 6 shows two simulations for different values of \check{H} and \check{W} , respectively. It can be seen that there is almost no difference in performance between the results, which

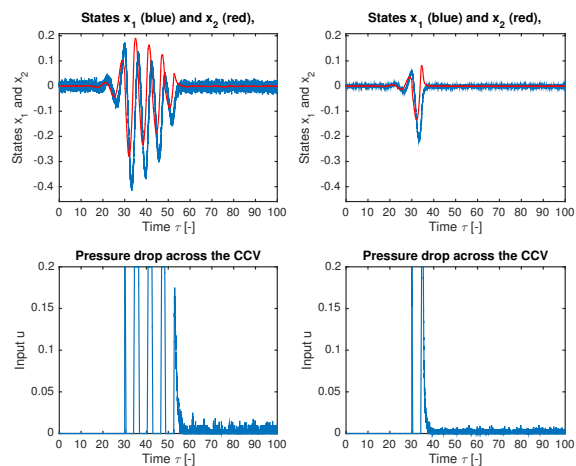


Fig. 5. Simulation results for $\check{k}_3 = 0.05$ ($\check{H} = 0.1$, $\check{W} = 1$), $\eta = 2$, $K_1 = 3$, $K_2 = 4$, $\alpha = 0.1$ and $\beta = 30$

indicates a small influence of the nonlinear feedback and thus robustness of the chosen control scheme.

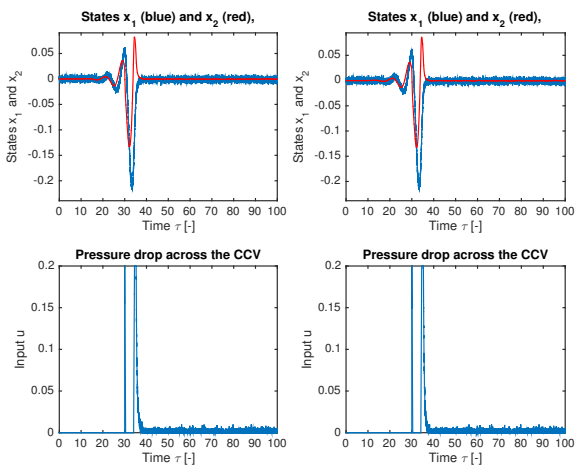


Fig. 6. Top left simulation: $\check{k}_3 = 0.5$ ($\check{H} = 1$, $\check{W} = 1$) and $\eta = 1$; top right simulation: $\check{k}_3 \approx 1.1662$ ($\check{H} = 0.1$, $\check{W} = 0.35$) and $\eta = 1$; for both simulations it holds: $K_1 = 3$, $K_2 = 4$, $\alpha = 0.1$ and $\beta = 30$

Figure 7 illustrates a comparison of two simulations with constrained and unconstrained input signals. These cases are only shown in order to highlight the theoretical investigations conducted in Section III. As can be seen, an unconstrained controller offers higher degrees of freedom with respect to the choice of the sector $[\alpha, \beta]$ and thus of the feedback gains K_1 and K_2 , which in this case are chosen larger than in the simulations presented in Figures 5 and 6, respectively. In the top left plot the case with a constrained input signal is demonstrated, whereas the unconstrained case is shown in the top right. It can be noticed that for the constrained case it is not possible to stabilize the system with high feedback gains in the linear feedback law (14) and thus it remains in surge. In the unconstrained case the system can be stabilized, however, the noise gets amplified by the large

feedback gains. The unconstrained case is not implementable in a real compression system, as such large and in addition negative pressure drops are not attainable with a CCV.

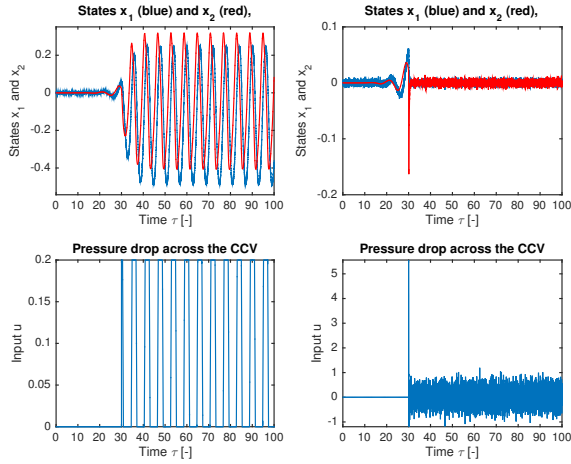


Fig. 7. Simulation results for $\tilde{k}_3 = 0.05$ ($\tilde{H} = 0.1$, $\tilde{W} = 1$), $\eta = 2$, $K_1 = 99$, $K_2 = 20$, $\alpha = 0.1$ and $\beta = 800$

V. CONCLUSIONS

In this paper we have shown that the feedback linearization methodology can be used to stabilize surge in a compression system. A robustness analysis based upon a sector nonlinearity feedback and a circle criterion investigation indicates that for deviations between the controller parameters \tilde{k}_i and those of the plant model k_i , the system can be stabilized and surge can be avoided. Even in the presence of added white Gaussian noise to the state derivatives \dot{x}_1 and \dot{x}_2 and the output y as well as imposing restrictions on the magnitude and slope of the control signal u , the feedback linearizing controller was able to stabilize the system. However, for large feedback gains and constrained input signals, the controller is not able to stabilize the system.

We point out that the parameters B and γ are assumed to be known exactly, which renders the robustness analysis only partial as it only holds for uncertainties in the parameters k_i . However, the values for B and γ could be estimated by e.g. adaptive techniques.

It must be mentioned that in all simulations the control signal goes back to the origin, or at least to a small environment around it (due to the added noise). This is due to the fact that the origin constitutes the equilibrium point. In a real compression system, however, we will obtain a stationary value for the control signal, which is constant and thus $\neq 0$.

APPENDIX: SIMULATION PARAMETERS

A_c	flow area	0.01 m ²
B	B-Parameter	≈ 0.8319
H	coefficient	0.18
L_c	length of ducts and compressor	3 m
U	compressor blade tip speed	80 m s ⁻¹
V_p	plenum volume	1.5 m ³
W	coefficient	0.25
a_s	speed of sound	340 m s ⁻¹
ψ_0, x_{1_0}	operating point for ψ , respective x_1	0.611, 0.533
ϕ_0, x_{2_0}	operating point for ϕ , respective x_2	0.6, 0.3
γ	throttle gain	0.768, 0.411

REFERENCES

- [1] C. J. Backi, J. T. Gravdahl, and E. I. Grøtli. Nonlinear observer design for a Greitzer compressor model. In *Proceedings of the 21st Mediterranean Conference on Control and Automation*, Chania, Crete, Greece, 2013.
- [2] B. Bøhagen, O. Stene, and J. T. Gravdahl. A GES mass flow observer for compression systems: Design and Experiments. In *Proceedings of the American Control Conference*, Boston, Massachusetts, USA, 2004.
- [3] B. de Jager. Rotating stall and surge control: A survey. In *Proceedings of the Conference on Decision & Control*, New Orleans, Louisiana, USA, 1995.
- [4] J. T. Gravdahl and O. Egeland. Compressor surge control using a close-coupled valve and backstepping. In *Proceedings of the American Control Conference*, Albuquerque, New Mexico, USA, 1997.
- [5] J. T. Gravdahl and O. Egeland. *Compressor Surge and Rotating Stall*. Advances in Industrial Control. Springer-Verlag, New York, 1999.
- [6] E. M. Greitzer. Surge and Rotating Stall in Axial Flow Compressors. Part I: Theoretical Compression System Model. *Journal of Engineering for Power*, 98:190–198, 1976.
- [7] A. Isidori. *Nonlinear Control Systems*. Springer Berlin, 3rd edition, 1995.
- [8] H. K. Khalil. *Nonlinear Systems*. Prentice Hall, New Jersey, 3rd edition, 2002.
- [9] A. Shiriaev, R. Johansson, A. Robertsson, and L. Freidovich. Output Feedback Stabilization of the Moore-Greitzer Compressor Model. In *Proceedings of the Conference on Decision & Control and the European Control Conference*, Seville, Spain, 2005.
- [10] A. Shiriaev, R. Johansson, A. Robertsson, and L. Freidovich. Criteria for Global Stability of Coupled Systems with Application to Robust Output Feedback Design for Active Surge Control. In *Proceedings of the Conference on Control Applications*, Saint Petersburg, Russia, 2009.
- [11] J. S. Simon. *Feedback stabilization of compression systems*. PhD thesis, Massachusetts Institute of Technology, Department of Mechanical Engineering, 1993.
- [12] N. Uddin and J. T. Gravdahl. Piston-actuated active surge control of centrifugal compressor including integral action. In *Proceedings of the 11th International Conference on Control, Automation and Systems (ICCAS)*, pages 991–996, Gyeonggi-do, South Korea, October 26–29 2011.
- [13] N. Uddin and J. T. Gravdahl. Introducing Back-up to Active Compressor Surge Control System. In *Proceedings of the 2012 IFAC Workshop on Automatic Control in Offshore Oil and Gas Production*, pages 263–268, Trondheim, Norway, May 31 – June 1 2012.

$$\text{Re}[\tilde{G}(j\omega)] = \frac{\omega^4 + \omega^2(K_1^2 - 2K_2 - \alpha - \beta - 2) + K_2^2 + K_2(\alpha + \beta + 2) + \alpha\beta + \alpha + \beta + 1}{\omega^4 + \omega^2(K_1^2 - 2K_2 - 2\alpha - 2) + K_2^2 + K_2(2\alpha + 2) + \alpha(\alpha + 2) + 1} \quad (24)$$

$$\omega_{1,2,3,4} = \pm \frac{1}{2} \sqrt{4 - 2K_1^2 + 4K_2 + 2(\alpha + \beta) \pm 2\sqrt{K_1^4 - 2K_1^2(2K_2 + \alpha + \beta + 2) + (\alpha - \beta)^2}} \quad (25)$$